QUANTITATIVE ASSESSMENT OF CORROSION IN AIRCRAFT STRUCTURES USING SCANNING PULSED EDDY CURRENT

Jay A. Bieber, Cheng-Chi Tai, and John C. Moulder

Center for Nondestructive Evaluation
Iowa State University
Ames, IA 50011

INTRODUCTION

Eddy current nondestructive testing techniques are used extensively in industry for detection of hidden cracks and corrosion in multi-layer conductive structures such as those found in aircraft. Most conventional eddy current techniques employ a probe coil excited with a continuous sine wave. The changes in the probe's impedance are detected (usually with an electronic bridge circuit) and displayed in real time on an impedance plane CRT display. Interpretation of the impedance-plane trajectories that result from scanning the probe over a defect is difficult; it involves a considerable amount of operator skill and knowledge and the equipment is sometimes difficult to set up and operate. We have developed an eddy current inspection system using the pulsed eddy current technique, which greatly reduces the possibility of operator errors and subjectivity in the quantitative interpretation of test results.

Pulsed eddy current techniques offer several advantages over conventional eddy current systems: First, because the probe coil is excited by a pulse, the average power that must be dissipated by the probe can be much less than for continuous waves of the same amplitude. Thus, higher drive levels may be used to provide the additional magnetic field strength to penetrate the specimen, which is necessary for detection of deeply buried flaws. Second, pulsed excitation injects a broad spectrum of frequencies into the test piece. This allows inspection of the entire depth of the specimen with just one pulse, which is much faster (~1 ms) and provides more information than the conventional single or multi-frequency approaches. Third, the time domain characteristics of the pulse may be analyzed and processed to yield results analogous to the A-, B-, and C-scans, with which NDT inspectors are familiar from ultrasonic methods. We have previously described in some detail how display of the results in this manner enhances the flaw discrimination capability of pulsed eddy current time-domain signals.[1]

Earlier theoretical and experimental work on pulsed eddy current testing has shown that it is possible to quantitatively determine metal loss in structures such as an aircraft lap-splice.[2,3] Much of this work was done on specimens designed to simulate corrosion in an aircraft lap-splice using machined flat bottom holes (FBH). In this paper we make use of a Scanning Pulsed Eddy Current (SPEC) prototype, Figs. 1 and 2, to demonstrate the quantitative capabilities of the system on specimens in which the metal loss is due to chemical corrosion. Details of the construction and operation of the instrument are described elsewhere.[4]

Review of Progress in Quantitative Nondestructive Evaluation, Vol 17
Edited by D.O. Thompson and D.E. Chimenti, Plenum Press, New York, 1998

EXPERIMENT

Figure 3 shows a schematic of the experimental arrangement used to model the pulsed eddy current experiments presented here. The coil that was used for our experiments was a 145-turn, right-cylindrical air-core coil, 9 mm in diameter. The coil was designed with a constant built in wear surface which gives a liftoff of approximately 0.16 mm. This geometry was chosen to simulate a two-layer aircraft lap-joint, with corrosion in the locations shown, and with some amount of air gap to simulate plate separation. The input to the coil is a 5.0 V, 120 Hz rectangular pulse, with a pulse length of 250 μs. The resulting current in the coil is detected by sensing the voltage drop in a 1 ohm resistor in series with the probe. The coil response is then digitized by a 16 bit, 1 MHz analog-to-digital converter. To obtain a pulsed eddy current flaw signal, the probe coil is first placed over a reference area on the sample that has no flaw. The coil response on this reference area (see Fig. 3) is then stored in memory and is subtracted from all subsequent incoming signals as the probe is scanned over the sample. The pulsed eddy current signal is the difference between the transient response of the coil over a flaw-free area, and an area that contains a flaw.

In our earlier experimental investigations using the SPEC instrument, the input to the probe coil was a 5.0 V, 500 μs unipolar square wave pulse, with a 50% duty cycle and a pulse repetition rate of 1 kHz. In the current version of the instrument, a microcontroller has been added, which allows software control of the pulse amplitude (from 0 - 10 V), repetition rate (70 Hz - 10 kHz), and duty cycle (0.5 to 99.5%). Using a typical probe design with the coil mounted in epoxy, we found that Joule heating of the probe becomes significant when the average power exceeds approximately 0.5 W. With a 12.5-ohm coil driven at the previous settings, the coil must dissipate 2 W.

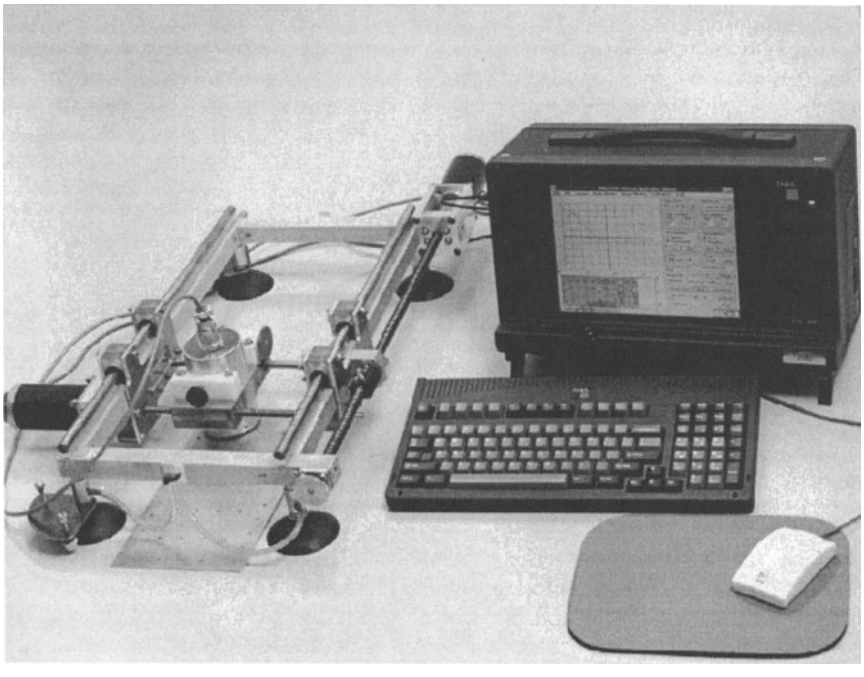

Figure 1. Photograph of the Scanning Pulsed Eddy Current instrument showing the portable x-y scanner and computer.

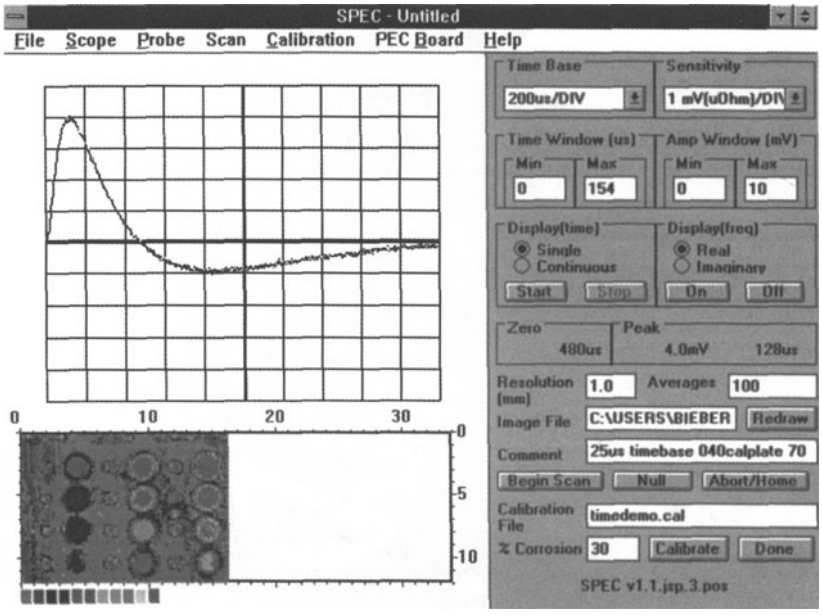

Figure 2. Scanning Pulsed Eddy Current instrument display, showing the instrument control panel on the right. The PEC waveform and C-scan display are shown at left.

With the ability to select the drive parameters we can now drive the same probe for 500 μS at 10.0 volts at a repetition rate of 100 Hz, thus reducing the average power by a factor of 5 to 0.4 watts while doubling the pulse intensity. The trade off, of course, is a slower data acquisition rate.

As shown in Fig. 4, the pulsed eddy current waveform has two main features that are used in flaw characterization. The first is the peak height, which is proportional to the amount of metal loss. The second is the zero-crossover point of the waveform, which contains information about the depth of the flaw in the structure. Waveforms are acquired continuously while the probe is scanned over an area of the sample using a portable two-axis scanner. Data acquired from 2-D scans are presented in a C-scan, pseudo-color image. For this article, the colors are rendered in a gray-scale format. To produce a C-scan image, the peak height of the PEC waveform is assigned a color corresponding to its amplitude at each x-y position of the probe. Peak amplitudes are assigned colors from a ten color look-up table. The range of amplitudes to be colorized is user selectable in the control software. Using this method, the amplitude sensitivity of the image can be increased or decreased, using the colors to represent any range of peak amplitudes desired.

The plot on the left in Fig. 5 shows a set of experimentally derived inversion curves measured on a model lap-joint consisting of two 1.5-mm aluminum plates. This plot shows the amplitude versus the time-to-zero-crossover for a range of flaw depths in the locations shown in the schematic below. The plots on the right are experimental PEC curves obtained on the same geometry for 30% metal loss in each layer. As is evident in the inversion plot, air gap, or simple plate separation, has the earliest time-to-zero crossover. This is due to the fact that, in this case, the original thickness of metal beneath the coil remains constant. This results in a lower inductance, and hence a faster rise and decay time for the probe coil, compared to when there is some degree of metal loss under the coil. Slightly later in time are the zero crossover points for flaws in the bottom of the top layer, followed by flaws in the top of the bottom layer, and finally bottom of the bottom layer.

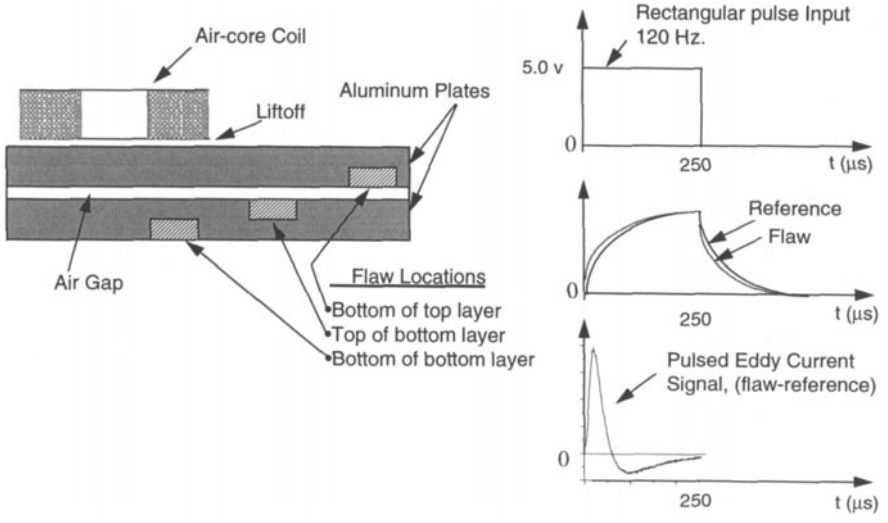

Figure 3. Schematic diagram of a pulsed eddy current experiment, showing the arrangement of the coil and specimen. The waveforms on the right show the coil current with and without flaw, which produce the pulsed eddy current difference signal.

The schematic at the bottom of Fig. 5 is of use in visualizing the relationship between flaw location and the slope of the inversion curves. In the case of corrosion in the bottom of the top layer, and the bottom of the bottom layer, greater metal loss results in a reduction of material between the coil and the metal-air interface. As illustrated by the arrows in the schematic, this results in slightly shorter eddy current diffusion times for deeper corrosion, as it advances toward the probe. This results in a negative slope of the inversion curve. In the case of corrosion in the top of the bottom layer, the metal-air interface remains fixed at a constant distance from the probe as corrosion increases, and therefore the inversion curve has a nearly vertical slope. The separation in time of flaws from different layers permits us to discriminate the location of corrosion based on time-gating. Time-gating is accomplished in the PEC software, as illustrated by the vertical bars in the display of Fig. 6. After a raw C-scan image has been acquired, the image may be redisplayed, plotting only those peak heights that have a zero crossover within this time window. The raw image contains all the peak heights, from the entire spectrum of zero crossover times possible during the pulse duration which, for these experiments, is 0 to 250μs.

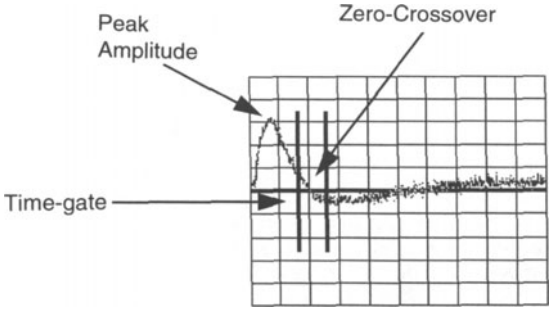

Figure 4. Scanning Pulsed Eddy Current signal display.

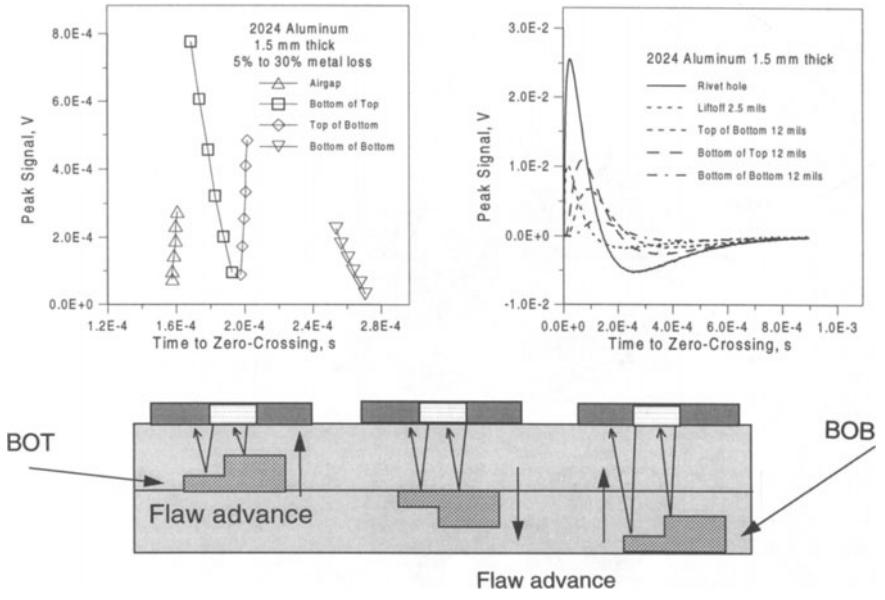

Figure 5. PEC experimental inversion chart and flaw waveforms for layer discrimination with the geometry shown for 1 mm thick 2024 Al plates.

To demonstrate the PEC instrument's ability to discriminate corrosion at different depths, a lap-joint calibration sample was constructed of two layers of 1.5-mm 2024 aluminum. Flat-bottom holes (FBH), 19 mm in diameter, were machined into the surface of each layer with depths of 5, 10, 20, and 30% of the thickness. Holes were also drilled through the sample to simulate fastener holes on 25.4 mm centers. Figure 6 shows the pulsed eddy current images obtained by scanning this sample. The top image represents the raw image, containing all peak heights possible. The time-gated image is the result obtained by setting the time gate minimum late enough to exclude the rivet holes which, because they are on the surface, have very early zero-crossover times. The lower time-gated images are the result of setting narrower time gates to include only those flaws from each individual layer. With the gate set for the times indicated, we are able to discriminate the flaws in the bottom of the top layer (right image), from the top of the bottom (middle image), and the bottom of the bottom layer (left image) as shown.

Using the ability to discriminate the location of flaws, the instrument may be calibrated to quantitatively determine the metal loss in the individual layers of the specimen. This is accomplished by creating calibration curves for each location, relating the amplitude of the peak signal to amount of metal loss. Figure 7 shows the same image data displayed after calibration, the colors in the lower time-gated images now indicate the metal loss at each location. As shown in Fig. 7, five different colors (shown here in shades of gray) are used to represent areas of corrosion in 5% increments, with red indicating 20% and greater metal loss. To calibrate the instrument, images such as those shown in Fig. 6. are first acquired on the calibration standard. Time-gating is then used to isolate the FBHs from each layer. The probe is then positioned directly over each FBH, recording the peak amplitude, and zero-crossing time. A table is then automatically generated from these values, which the software uses to generate calibration curves for each layer by fitting a polynomial to the data. The software then assigns a color to each peak amplitude in the image, using the polynomial fit to determine the metal loss. Figure 8 shows a plot of the calibration curves obtained in this way from the 1.5-mm lap-splice calibration standard. In this case, a 2nd degree polynomial fit closely approximates the experimental data from each of the three layers.

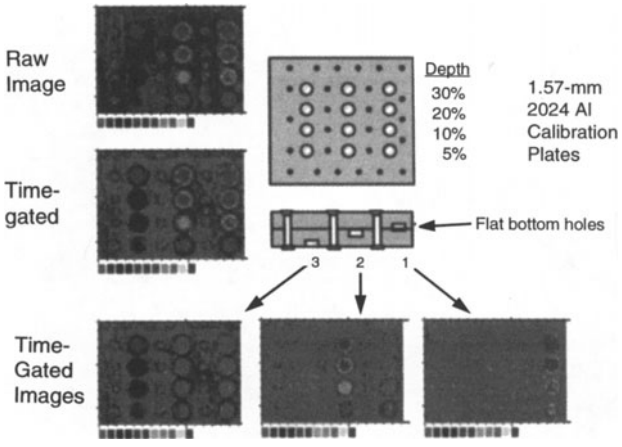

Figure 6. PEC image of 1.57-mm lap-joint calibration standard, time-gated to discriminate the flaws from each layer.

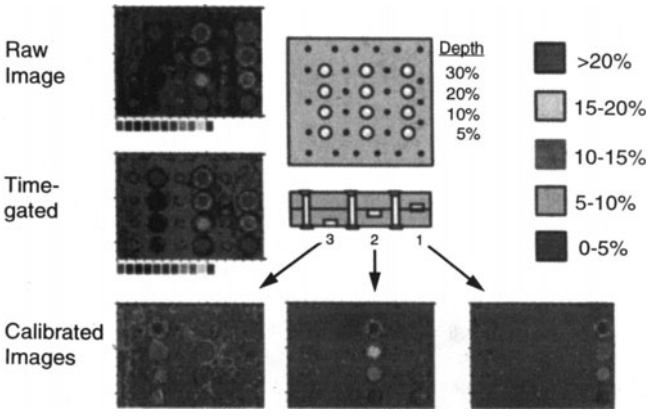

Figure 7. SPEC image of 1.57 mm lap-joint calibration standard displayed in calibration mode.

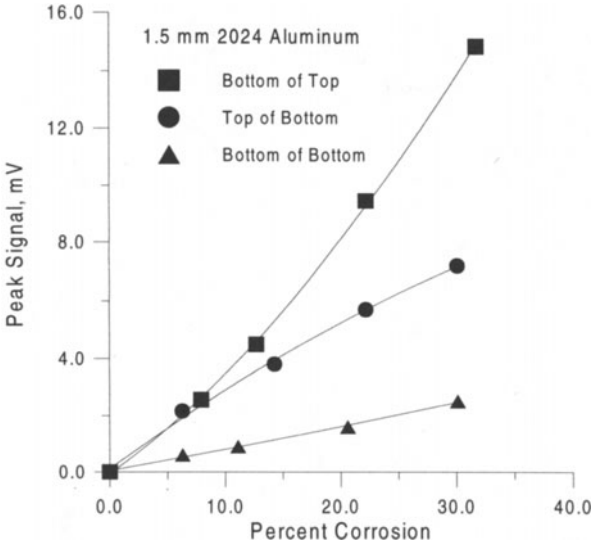

Figure 8. Calibration curves from 1.57 mm calibration standard.

This calibration method was then tested on laboratory specimens of aluminum that were chemically corroded in a salt-spray chamber for a period of several weeks. The photograph in Fig. 9 shows the irregularly shaped corrosion areas that were produced in one specimen. The uncorroded areas were masked from the salt spray using a removable masking paint. The image on the right is the scanning pulsed eddy current image of this specimen displayed in the calibrated mode. The corrosion free area at point "n" was chosen to acquire the reference signal. Individual pulsed eddy current peak amplitudes were recorded at points "a" through "h", with the percent metal loss determined from the calibration curves in Fig. 8. The corroded surface was placed in each of the three locations, bottom of top (BT), top of the bottom (TB), and the bottom of the bottom (BB) plate. A corrosion-free sheet of aluminum was used as the second layer of the lap-splice. In this image, as before, the colors are binned into 5% increments, with red indicating a metal loss of 20% and greater. The image shown here was acquired with the corrosion at the bottom of the top layer. Quantitative results for each of the three locations of corrosion are tabulated in Fig. 9, along with corrosion depths measured by micrometer (MEAS), and by immersion ultrasound (UT). Because of the pitting nature of the corrosion, and also the difficulty in removing all of the corrosion product from the specimens, the values measured by micrometer are likely to be less than the actual metal loss. The PEC results for each of the corrosion locations agree reasonably well within a range of approximately +/- 2 percent, the only exception being point "a" on the bottom of the bottom layer.

CONCLUSIONS

We have demonstrated the ability of a newly developed prototype scanning pulsed eddy current system to quantitatively determine the metal loss in a simulated aircraft lap-splice. The instrument can detect and discriminate corrosion in multi-layer metal aircraft structures. Using the computer controlled calibration routine in the instrument's software, the instrument is capable of producing a quantitative C-scan image. The calibration and display of quantitative results in this way should reduce the possibility of operator subjectivity or error in the reporting of test results.

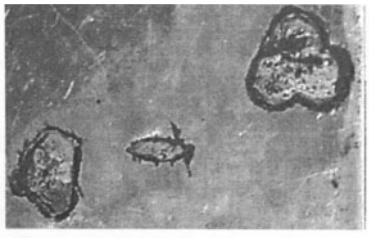

Photograph of Corrosion Specimen

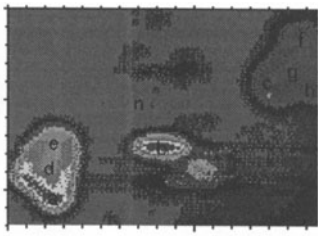

Calibrated PEC image

Point	BT%	TB%	BB%	UT	MEAS.
a	25.2	24.1	29.3	24.8	20.6
b	24.5	25.8	27.0	20.6	20.6
c	12.9	15.2	13.8	14.3	11.1
d	18.5	19.9	22.2	20.6	17.6
e	18.5	20.4	22.2	15.5	11.3
f	11.1	14.4	12.4	8.0	5.0
g	12.3	15.7	13.8	14.3	8.0
h	13.9	15.2	13.8	14.3	9.6

Figure 9. Quantitative results on specimen corroded in a salt-spray chamber.

ACKNOWLEDGMENTS

This work was supported by the FAA Center for Aviation Systems Reliability program at the Center for NDE at Iowa State University and was supported in part by AFOSR grant No. F49620-93-1-0439DEF and by the Federal Aviation Administration under Grant No. 95-G-018.

REFERENCES

1. J. A. Bieber, S. K. Shaligram, J. H. Rose, and J. C. Moulder, "Time-gating of pulsed eddy current signals for defect characterization and discrimination in aircraft lap-joints," in Review of Progress in Quantitative Nondestructive Evaluation, Vol. 16B, edited by D. O. Thompson and D. E. Chimenti, (Plenum, New York, 1997) p. 1915-21.
2. J. C. Moulder, M. W. Kubovich, E. Uzal, and J. H. Rose, "Pulsed eddy-current measurements of corrosion-induced metal loss: theory and experiment," in Review of Progress in Quantitative Nondestructive Evaluation, Vol. 14B, edited by D. O. Thompson and D. E. Chimenti, (Plenum, New York, 1995) p. 2065-72.
3. J. H. Rose, E. Uzal, and J. C. Moulder, "Pulsed eddy-current characterization of corrosion in aircraft lap splices: Quantitative modeling,", in Superconductive Devices and Circuits, edited by Robert A. Buhrman; John T. Clarke; Ken Daly; Roger H. Koch; Jerome A. Luine; Randy W. Simon, SPIE Vol. 2160, (SPIE, Bellingham, 1994) pp. 164-176.
4. J. C. Moulder, J. A. Bieber, W. Ward III, and J. H. Rose, "Scanned pulsed-eddy-current instrument for non-destructive inspection of aging aircraft," in Nondestructive Evaluation of Aging Aircraft, Airports, and Aerospace Hardware, edited by R. D. Rempt and A. L. Broz, SPIE Vol. 2945, (SPIE, Bellingham, 1996) pp. 2-13.